The Behavior of a Reactor Pressure Vessel Nozzle Under Pressurized Thermal Shock Loading

M. Klein, G. E. Neubrech
Kernforschungszentrum Karlsruhe, Karlsruhe, FRG
E. Roos
MPA, Universität Stuttgart, Stuttgart, FRG

INTRODUCTION

The integrity of the reactor pressure vessel (RPV) must be guaranteed for all failure and loading conditions which may be possible during operation and accidents. The impact of internal pressure and long time thermal shock (due to cold water flow) on postulated cracks at a nozzle is to be considered as the worst case. In a loss-of-coolant accident with injection of cooling water such loads are to be expected. It was the essential aim of these investigations to qualify the knowledge of the temperature gradients, of the flow paths in the medium, of the stresses in the structure, of the crack loading and of the crack growth rate of the RPV-material.

EXPERIMENTAL CONDITIONS

The investigations were performed at the HDR test facility at Karlstein near Frankfurt/Main (the decommissioned "superheated steam reactor"), in the Phase II of the "project HDR safety program" (PHDR) by the Karlsruhe Nuclear Research Centre (KfK). The object of the investigation, the nozzle A_2 of the RPV, with its main dimensions is shown in Fig. 1. The RPV was produced of the steel 23 NiMoCr 3 6 with a cladding on the inside. In order to apply the thermal shock loadings it is possible to inject cold water into the RPV under steady state conditions (310°C, 10.6 MPa).
At the corner of the nozzle A2 thermal shock cracks were produced by 3700 cyclic thermal shocks. The water contained about 8 ppm O_2 as the "worst case" for corrosion attack. On the one hand these tests served for investigations of crack formation and crack propagation, on the other hand it was an aim to qualify nondestructive on-line and off-line testings which documented the crack propagation during the tests (Klein et al, 1987). Finally the cracks were loaded with two pressurized thermal shocks (PTS).
In the first test, THEL I, a stratification of cold and hot water was produced in the nozzle by means of a free cold water injection. In the second test, THEL II, the nozzle was cooled rotational symmetrical by the device in Fig. 1. During the two tests temperatures, strains and the crack mouth opening displacement (CMOD), were measured at the inside and at the outside of the nozzle.

RESULTS

After about 1000 thermal shocks ($\Delta T \geq 250°C$) with a strain rate of about 0.5% crack formation was detected in the cladded nozzle. Fig. 2 shows, as the result of the dye penetration testing, the large field of cracks after 3700 cycles. Potential drop examination

after 3000 cycles indicated the existence of deeper cracks at the 167° and 180° positions, Fig. 3 a+b. These dominating cracks, which were located in a small area, can be considered as separate, single cracks in three-dimensional elastoplastic finite-element analyses only at tremendous expenditure. For this reason, an enveloping equivalent crack in the 180° position was assumed, Fig. 3 c. In the light of the experience accumulated in the first tripan removed from the nozzle after a former test period, the crack depth measurements by potential drop tests had been 20% too low compared to the fractographic findings. Therefore to the crack depth after 3700 thermal shock cycles 20% was added. This idealized crack has a maximum depth of 28 mm and a length of 140 mm.

In the first pressurized thermal shock, THEL I, a stratification of cold and hot water occurred in the nozzle. Fig. 4 shows the measured temperatures. The lower part of the nozzle (85 mm level of the 200 mm diameter) was cooled down to 50°C (curve 2/THEL I) for half an hour. The upper half of the nozzle remained hot (curve 1/THEL I). During this time the temperature at the crack tip (curve 3/THEL I) remained at about 100°C, which is the beginning of the upper shelf of the material thoughness. The maximum loading for the cracks in the nozzle was reached with 0.3% circumferential strain (curve 1/THEL I, Fig. 5) within the first five minutes. After that the strain decreased to 0.26% and remained constant for the rest of the test.
In the second pressurized thermal shock, THEL II, the complete inner surface of the nozzle was cooled down to 50°C, (Fig. 4 curve 1 and 2/THEL II).
The safety analysis for these tests (Roos et al, 1988) demanded that the experiment has to be stopped, if the temperature at the deepest point of the crack (curve 3/THEL II, Fig. 4) has reached 80°C. In the test this temperature was reached after 16 minutes.
The maximum loading for the axial cracks was reached with 0.4% circumferential strain (curve 1/THEL I in Fig. 5) within the first five minutes. To compare the loadings of the nozzle in both tests the equivalent strains for THEL I and II (Fig. 6) may be approximately calculated from the measured strains in Fig. 5 according to

$$\varepsilon_v = \sqrt{\varepsilon_1^2 + \varepsilon_2^2 + 0{,}125\,\varepsilon_1\varepsilon_2}.$$

In THEL II the maximum loading for the deepest crack was reached with a CMOD of about 0.2 mm after two minutes and decreased constantly after that, Fig. 7.
Advanced calculations made by means of the finite element method were extended by fracture mechanics evaluations, thus allowing the determination of the time dependent temperature fields, stress distributions, J-integral values and CMOD caused by thermal shocks on threedimensional geometry configurations (Roos et al, 1988, and Kußmaul et al, 1989). The crack contour used in the calculation is shown in Fig. 3c.
It is striking to see the partly good agreement up to maximum loading in Fig. 7 between the calculated an the measured CMOD, as a too deep enveloping crack had been calculated for the 180° position whereas in reality, there were two cracks at 167° and 180°, Fig. 3. The relatively bad agreement between the calculation and the measurement after the maximum load can be traced back to the CMOD measurement technique by means of strain gages, as load relief after a plastic deformation falsify the measured values due to buckling. On-line monitoring of the nozzle by means of a stationary potential probe did not reveal any indications of stable crack

growth. However, the high-amplitude acoustic emission readings indicate crack growth. After the whole A2 nozzle had been removed, the crack region at the 167° and at the 180° position was subjected to a detailed fractographic advanced examination, indications of minimal stable crack growth were found in the region of the crack tip.
Comparison of the fracture surface with the contour of the calculated crack shows the real crack size to have been clearly smaller, Fig. 8. There are uncertainties in the non-destructive testing.
The comparison of the measured and calculated CMOD in Fig. 7 shows, that the calculation is not on the save side in all cases. Especially in this case a deeper crack than in the reality was used in the analysis.

CONCLUSIONS

In the region of a nozzle of the RPV, cyclic thermal shock loads with temperature diferences of ΔT = 260 K were applied to produce cracks. These cracks were subjected to two long thermal shock loads with $\Delta T \sim 260$ K under full serice pressure of p = 10.6 MPa. The first shock gives a relation to the reality. The second shock with a conducted rotational symmetrical cooling, which results in high stresses, was analysed by finite elements. The comparison of the equivalent strains shows, that, as expected, the loading for the nozzle was higher in the second shock. The calculated CMOD seems to be in a good agreement with the measurements. But the non-destructive testing had overestimated the real crack depth.

REFERENCES

Klein, M., Neubrech, G., Walte, F. (1987)
Fracture Mechanics Evaluation on the HDR AE Thermal Shock Trials, Smirt-9 Pre-Conference Seminar on Acoustic Emission, Stuttgart, 12.-13. August 1987.

Kußmaul, K., Roos, E., Stegmeyer, R., Katzenmeier, G. (1989).
Pressurized Thermal Shock Loading of HDR RPV-Nozzle and Cylindrical Wall. Proc. 10th SMIRT, Anaheim, California, August 14-18, 1989.

Roos, E., Stegmeyer, R., Diem, H., Klein, M., Neubrech, G. (1988).
Untersuchungen zur Wandbeanspruchung und zum Rißverhalten am Reaktordruckbehälter unter Langzeit-Thermoschockbelastung.
12. Statusbericht des PDHR im Kernforschungszentrum Karlsruhe 8.12.1988, Arbeitsbericht Nr. 05.43/87.

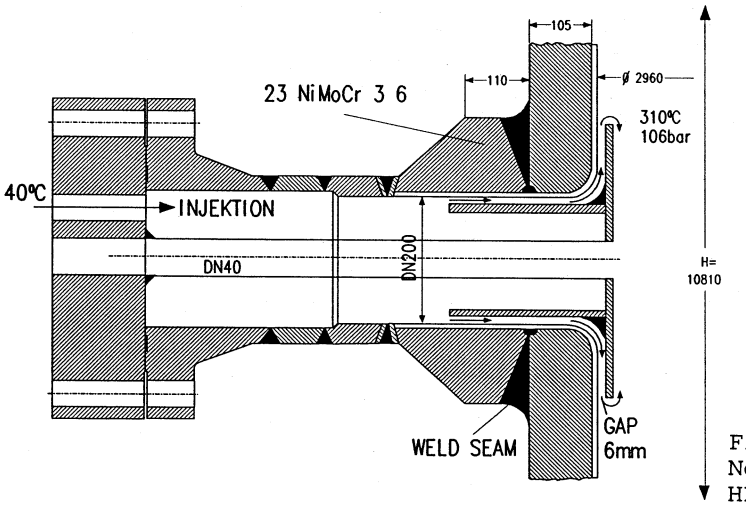

Fig. 1 Test setup: Nozzle A2 of the HDR RPV

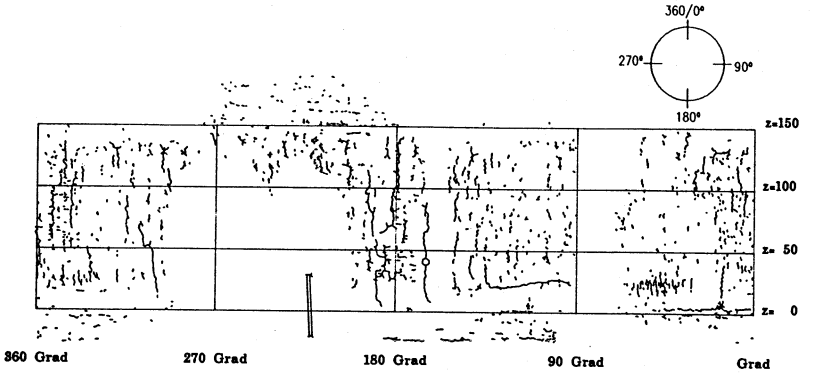

Fig. 2 Dye penetration test of the inner surface of the nozzle A2.

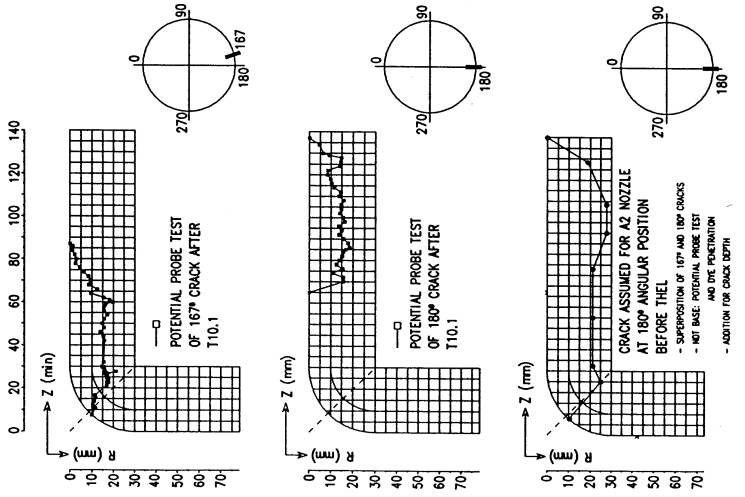

Fig. 3 Non-destructive test information and assumed crack shape for the analysis of the crack in the A2 nozzle.

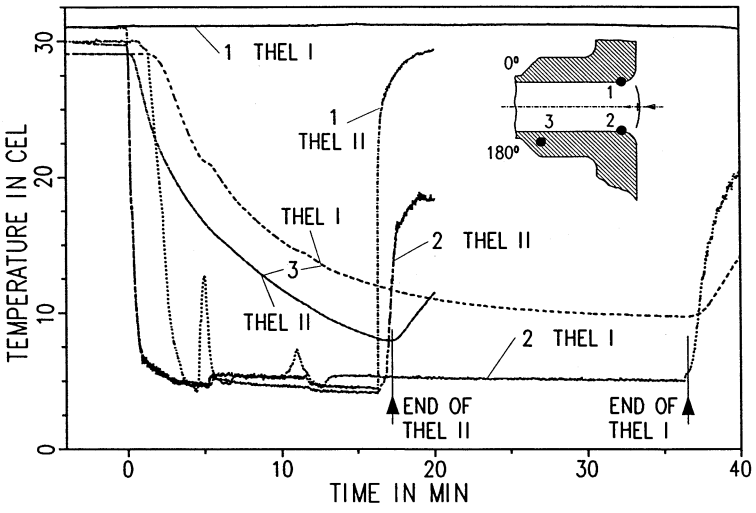

Fig. 4 Comparison between the measured temperatures of THEL I and II.

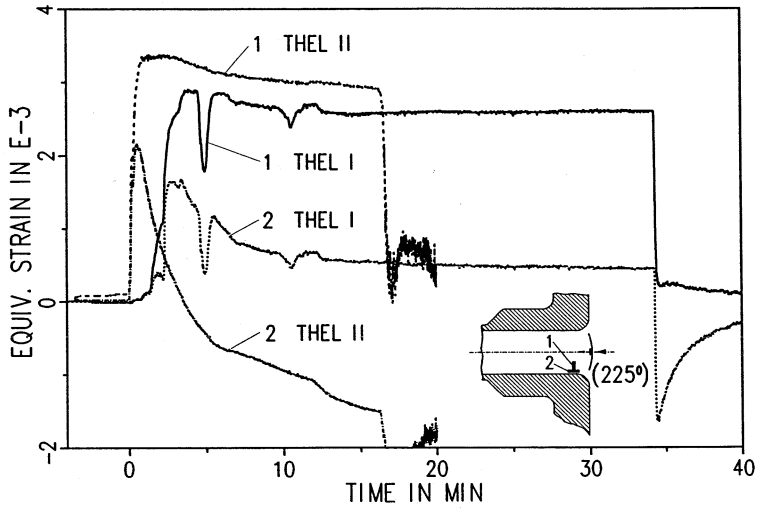

Fig. 5 Comparison between the measured strains of THEL I and II.

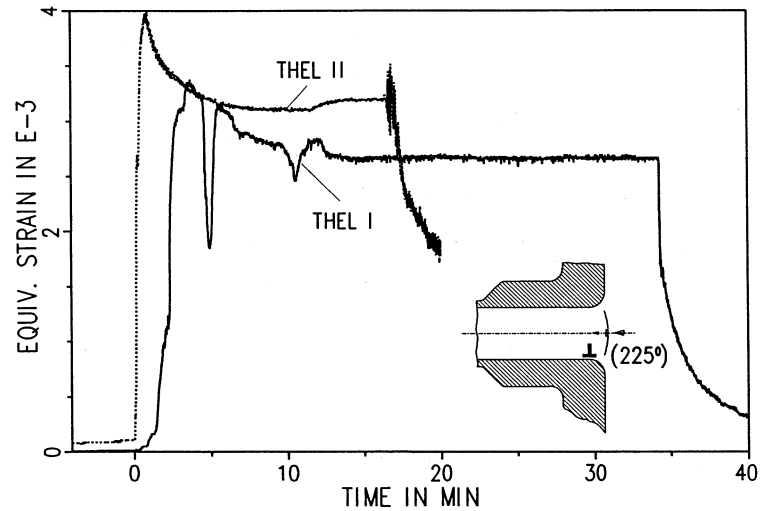

Fig. 6 Comparison between the equivalent strains of THEL and II.

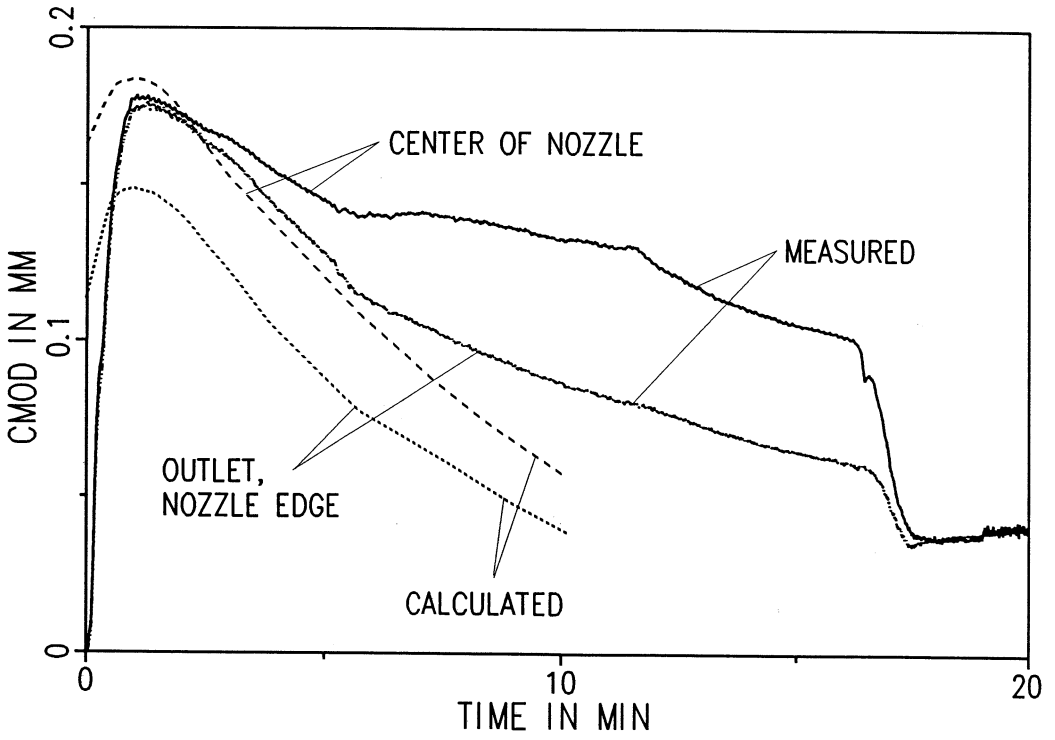

Fig. 7 Comparison between the measured and the calculated CMOD.

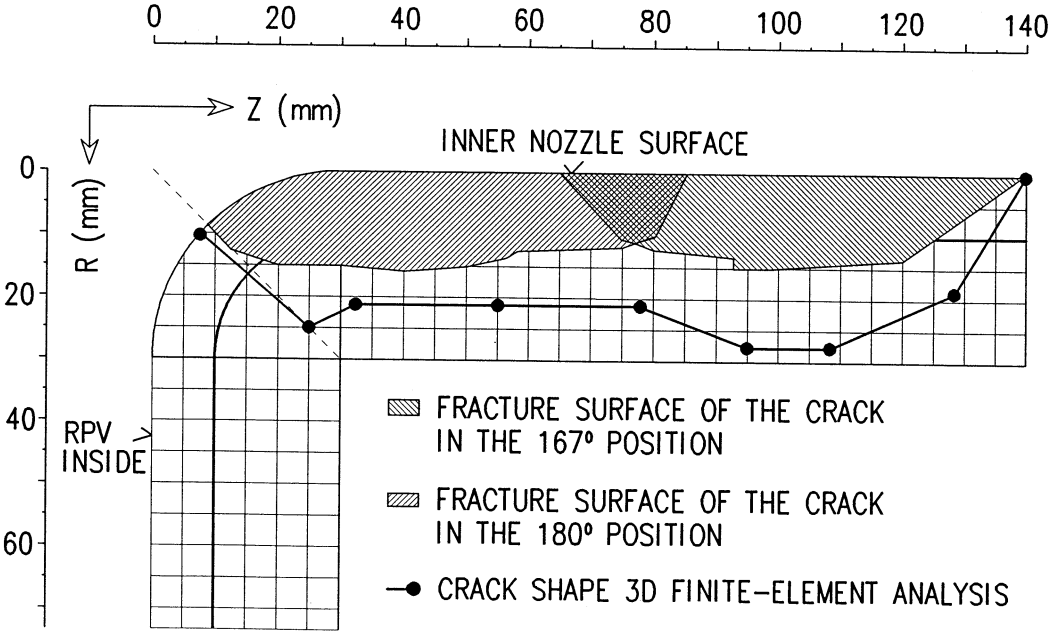

Fig. 8 Fracture surfaces of the cracks in the 167° and 180° positions as compared to the assumed crack contour